DESIGN OPTIMIZATION OF STEEL MOMENT FRAMES UNDER EXTREME EARTHQUAKE LOADING

Yanglin Gong

Department of Civil Engineering, Lakehead University, Thunder Bay, Ontario, Canada, P7B 5E1
Tel.: +1-807-343-8412; fax: +1-807-343-8928.
(Corresponding author: E-mail : yanglin.gong@lakeheadu.ca)

Received: 3 May 2005; Revised: 26 May 2006; Accepted: 5 June 2006

ABSTRACT: The paper presents a design optimization method for steel moment frames under extreme earthquake loading. Seismic responses of the structures are evaluated using a nonlinear pushover analysis procedure. Minimum structural cost and uniform heightwise ductility demand are identified as the design objectives. Roof and interstory drifts are taken as design constraints. Strong-column weak-beam requirement is treated as additional constraints for special moment frames. The sensitivities of inelastic displacements are employed to explicitly formulate the objective functions and constraints in terms of member sizing variables. A dual method is then used to search for an optimal design solution. The proposed design methodology is illustrated for a nine-story moment frame example.

Keywords: structural optimization; seismic design; steel moment frames; pushover analysis; ductility; design sensitivity analysis

1. INTRODUCTION

For the seismic design of building frameworks, modern seismic provisions, such as NEHRP [1] and NBCC [2], generally employ a seismic force reduction factor to reduce elastic spectral demand to the design level to account for the ductility of structures. Structures with more ductility are designed for lower forces than less ductile structures, as ductile structures are considered capable of resisting demands that are significantly greater than their elastic strength limit. The advantage of using reduced force for design is that this force is suitable for use with an elastic structural analysis. Obviously, this design procedure is unable to evaluate the true strength of structures at the ultimate limit state. If a structure's reserve strength beyond the design level is significantly less than that implicitly assumed, the performance of the structure is unlikely to be satisfactory during severe earthquake hazards. Furthermore, inelastic displacements cannot be calculated from the results of an elastic analysis. As an approximation, seismic provisions usually use displacement amplification factors to predict the maximum inelastic displacements from the elastic displacements corresponding to the reduced seismic force. However, it was found that the values of the force reduction and displacement amplification factors adopted by modern seismic provisions, such as NEHRP [1] and NBC [2], were often far from agreement with reality [3].

Steel moment frames designed based on modern seismic provisions are deemed to deform far into inelastic region during severe earthquake hazards. They are designed using a large force reduction factor since they are regarded as being among the most ductile systems. Steel moment frames are anticipated to develop their ductility through the development of yielding in beam-column assemblies at the connections. This yielding may take the form of plastic hinge in the beams and in the columns, plastic shear deformation in panel zones, or through a combination of these mechanisms. Thus an inelastic analysis to evaluate the seismic demands on steel moment frames is essential in order to assess the true structural performance.

A major challenge in designing steel moment frames is to provide a similar ductility demand in all stories such that weak or soft story can be avoided when the structure undergoes tremendous plastification or at the incipience of collapse. Structures with inappropriate heightwise distribution

of strength and stiffness usually exhibit large deformation concentration at a soft or weak story, which might lead to collapse of the buildings. Chopra [4] studied the ductility demands for several shear buildings, which were designed conforming to the 1997 Uniform Building Code, and found that in most of cases the ductility demand in the first story was several times greater than that of all the other stories. Without using an inelastic analysis, the objective of designing building frames for a uniform ductility demand will not likely be accomplished.

Seismic design approaches based on inelastic structural analyses are greatly needed for further development of modern seismic provisions. This is reflected by the adoption of two nonlinear analysis procedures (i.e., pushover analysis and response-history dynamic analysis) by FEMA-356 [5] as major tools to evaluate seismic demands for building rehabilitations. Among these two nonlinear procedures, pushover analysis is often seen to be the more attractive method due to its relative simplicity. A pushover analysis is basically a step-by-step plastic analysis for which lateral loads of invariant relative magnitude are applied to a building structure and progressively increased until a target roof displacement or a design base shear is reached. Pushover analysis can determine the ultimate strength as well as trace the sequence of yielding events of structures with satisfactory accuracy when it is used for predicting seismic responses of low-rise to mid-rise buildings where the influence of higher modes is insignificant. Extensive research works on pushover analysis were conducted by Krawinkler and Seneviratna [6], Hasan et al. [7], Elnashai [8], among others.

Structural design is traditionally accomplished by a trial-and-error procedure, which is laborious task and cannot guarantee an optimal design. Particularly, seismic design using a pushover analysis procedure is very computationally intensive due to the inelastic nature of the analysis method. Structural optimization [9, 10], which concerns obtaining the optimal design solution for a given structure while satisfying code- and designer-specified restrictions, provides a computer-based tool that may replace conventional design approaches with a systematic design process.

The research associated with structural optimization for earthquake loading using nonlinear analysis techniques is growing recently. Ganzeri et al. [11] employed a pushover analysis to design reinforced concrete portal frames in the context of performance-based seismic design. Chan and Zou [12] proposed an optimization algorithm for reinforced concrete structures. They decomposed the design process into two single-criterion phases. The first phase was an elastic design optimization in which the cost of concrete is minimized subject to elastic displacement constraints due to a minor earthquake. The second phase was minimizing the cost of steel reinforcement subject to constraints on inelastic displacements evaluated using a pushover analysis procedure. Liu et al. [13] and Xu et al. [14] adopted a pushover analysis to predict seismic responses for a multiobjective performance-based design of steel moment frames. Though not directly concerning seismic design, other structural optimization studies involving nonlinear analysis can be found in works by Haftka [15], and Foley and Schinler [16].

In this study, a design optimization algorithm is developed for planar steel moment frames under extreme earthquake hazards. Structural design is defined herein as a process of proportioning sectional size of steel members to satisfy performance criteria under the assumption that the geometric layout of moment frames is predefined and fixed throughout the design process. The design objectives are minimum structural cost and uniform ductility demand. Drift constraints, strong-column weak-beam and member sizing requirements are imposed to the design problem. A recently developed pushover analysis technique by Hasan et al. [7] is employed to predict the seismic demands for steel moment frames. A nine-story rigid moment frame is adopted as a design example to illustrate the applicability and effectiveness of the developed design methodology.

In a companion study by the author [17] on design optimization of steel moment frames, minimum structural cost was taken as the explicit design objective while another objective of uniform ductility was achieved indirectly by manipulating interstory drift constraints. Since no ductility objective function was used explicitly, the design method did not appear to guarantee that the obtained design was always a uniform ductility design. This paper, therefore, is a further development of the previous study [17].

2. PUSHOVER ANALYSIS UNDER EARTHQUAKE LOADING

The adopted pushover analysis procedure is an elastic-plastic hinge method. The composite finite element (see Figure 1), which consists of two potential plastic-hinges at the ends of an elastic beam-column, was developed for nonlinear analysis of planar steel moment frames. The corresponding stiffness matrix **K** for the composite element is found as, [7],

$$\mathbf{K} = \mathbf{S}\,\mathbf{C}_s + \mathbf{G}\,\mathbf{C}_g \tag{1}$$

where: **S** is the standard stiffness matrix for an elastic frame member [18]; $\mathbf{C}_s$ is a correction matrix expressed in terms of plasticity-factors p that characterize the degradation of flexural stiffness due to post-elastic deformation [7]; **G** is the standard geometric stiffness matrix [18]; $\mathbf{C}_g$ is the corresponding correction matrix formulated as a function of plasticity-factors p [7]. The plasticity-factor p of the plastic hinge at each member end is defined as,

$$p = \frac{1}{1 + 3EI/R^p L} \tag{2}$$

where R^p is the instantaneous rotational stiffness of the potential plastic hinge there, and L and EI are the length and elastic flexural stiffness of the member, respectively. For a fully elastic section $R^p = \infty$ and $p = 1$, for a fully plastic section $R^p = 0$ and $p = 0$, while for a partially plastic section $0 < p < 1$.

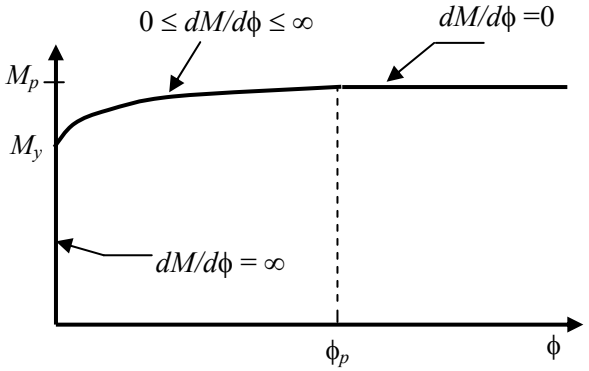

Figure 1. Composite Planar Beam-column Element

2.1 Single Stress Yield Condition

The moment-rotation (M-ϕ) relation that characterises the nonlinear variation in the post-elastic rotational stiffness R^p of a plastic-hinge section under increasing moment (see Figure 2) is taken to be, [7],

$$M(\phi) = M_y + \sqrt{(M_p - M_y)^2 - \left[(M_p - M_y)(\phi_p - \phi)/\phi_p\right]^2} \tag{3}$$

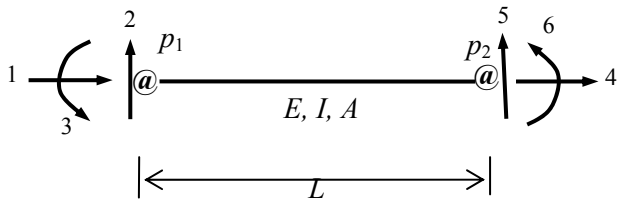

Symbol @ represents a plastic hinge

Figure 2. Post-elastic Moment-rotation Relation for Plastic Hinges

where $M_y=S\sigma_{ye}$ and $M_p=Z\sigma_{ye}$ are the known first-yield and fully-plastic moment capacities of the member section, respectively (S and Z are the elastic and plastic section moduli, respectively, and σ_{ye} is the expected yield stress of steel material.), and ϕ is the extent of post-elastic rotation occurring somewhere between first yielding ($\phi=0$) and full plastification ($\phi=\phi_p$) of the cross-section. From Eq. (3), the post-elastic moment varies in the range $M_y \le M(\phi) \le M_p$ as the plastic rotation varies in the range $0 \le \phi \le \phi_p$, as shown in Figure 2. Upon differentiating Eq. (3) with respect to ϕ, the post-elastic rotational stiffness of the section is found as,

$$R^p = \frac{dM(\phi)}{d\phi} = \frac{(M_p - M_y)^2(\phi_p - \phi\ )}{\phi_P^2\sqrt{(M_p - M_y)^2 - \left[(M_p - M_y)(\phi_p - \phi)/\phi_p\right]^2}} \quad (0<\phi\le\phi_p) \tag{4}$$

The incremental load-step method [18] is adopted to conduct the pushover analysis. The first step load is taken arbitrarily small so that the structure remains elastic. The structural global stiffness matrix is initially formed from member stiffness matrices defined by Eq. (1) by setting all plasticity-factors equal to unity (p=1*)* in matrices $\mathbf{C}_s$ and $\mathbf{C}_g$. After each incremental load, the structural tangent stiffness matrix is updated for member stiffness matrices modified by plasticity-factors p found from Eq. (2).

2.2 Combined Stress Yield Condition

The Section 2.1 is extended to the combined bending moment M and axial force N for members of planar frameworks. The reduction in the moment capacity of a member cross-section due to the presence of axial force can be account for through the following interaction equation, [19],

$$\frac{1}{f_s} \le \frac{M}{M_p} + \left[\frac{N}{N_p}\right]^a \le 1 \tag{5}$$

where A is the cross-section area and $N_p=A\sigma_{ye}$ is the fully-plastic axial force capacity; $f_s=M_p/M_y=Z/S$ is the section shape factor. The exponent a depends on the section shape (e.g., a =2 for a rectangular section).

For this study, a=1 was used for the sake of illustration. Note that a linear interaction curve is conservative and applicable for both tensile and compressive axial forces [20]. The two bounds of Eq. (5) define the plasticity zone are shown in Figure 3. Here, assuming that the ratio M/N remains invariant in the post-elastic response range for the combined stress case when both $M\neq0$ and $N\neq0$, identical satisfaction of the lower bound of Eq. (5) at generic point O_y in Figure 3 corresponds to first-yield behavior occurring at the reduced yield moment level $M_y^r=M_p/\xi f_s$ (where

$\xi=M_y/M_y^r=M_p/M_p^r$ and $\xi>1$), while identical satisfaction of the upper bound of Eq. (5) at related point O_p in Figure 3 corresponds to fully-plastic behavior occurring at the reduced plastic moment level $M_p^r=M_p/\xi=f_sM_y^r$. Upon replacing M_y and M_p with the reduced moments M_y^r and M_p^r, Eqs. (3) and (4) then respectively define post-elastic moment-rotation and flexural-stiffness relations that account for the influence of axial force on bending moment capacity of member sections, and the post-elastic analysis can proceed exactly as for the single stress yield condition in Section 2.1.

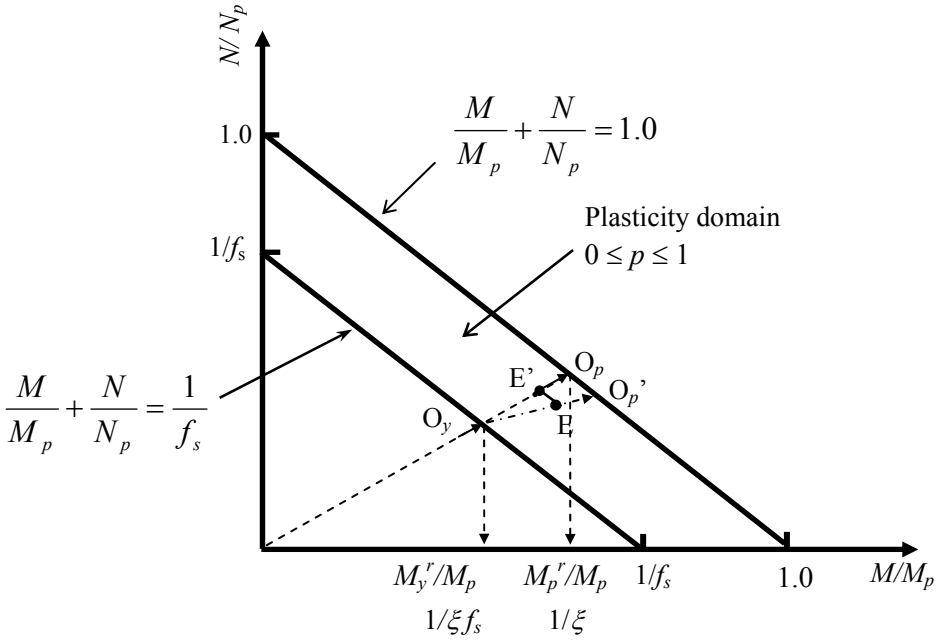

Figure 3. Combined Action of Bending Moment and Axial Force

The assumption that the ratio M/N remains constant in the post-elastic response range in Figure 3 is not always the case in reality. For example, sectional forces may follow the line O_y--O_p' in Figure 3, which results in a negative argument for the square root term in Eq. (5). To overcome such a computational difficulty, an equivalent moment concept is introduced by projecting the real bending moment to line O_y--O_p (e.g., bending moment at point E in Figure 3 is projected to point E' by drawing a line parallel to the yielding boundary through the moment point). Then, M in Eq. (5) is replaced by an equivalent moment M_{eq} found from the similarity of triangles shown in Figure 3; i.e., assuming a=1 for Eq. (5):

$$\frac{M_y^r}{M_{eq}}=\frac{1/f_s}{\zeta} \qquad \therefore \quad M_{eq}=M_y^r\,\zeta\,f_s \tag{6}$$

where $\zeta=(N/N_p+M/M_p)$. In the above transformation, M_{eq} has the same sense as the original bending moment.

The pushover analysis is performed for constant gravity loads and monotonically increasing lateral inertial loads. Seismic demands are equal to the structural responses at the load step when the base shear force is equal to the design base shear, which is determined according to an inelastic design spectrum. The design base shear can be evaluated as:

$$V_b=\frac{S_a}{g}W \tag{7}$$

where: S_a (in the unit of g) is the spectral response acceleration corresponding to a specified extreme earthquake hazard, e.g., a 2% probability of exceedance in 50-year earthquake event; g is the gravitational acceleration; and W is the seismic weight of the framework. Without loss of generality, the spectral response acceleration S_a curve for this study is taken as, [4],

$$S_a = \begin{cases} S_s & T \le T_0 \\ \dfrac{S_1}{T} & T > T_0 \end{cases} \tag{8}$$

where: T is the elastic fundamental period of the structure in seconds; T_0 is the period at which the constant acceleration and constant velocity regions of the response spectrum intersect for the design earthquake; and S_s and S_1 are corresponding short-period and one-second-period response acceleration parameters, respectively. The design spectrum has already accounted for target ductility.

The design base shear V_b is applied to the structure according the load pattern defined by, [5],

$$\mathbf{P}_l = V_b \begin{Bmatrix} C_{v,1} \\ C_{v,2} \\ \cdots \\ C_{v,n_s} \end{Bmatrix} = V_b \cdot \mathbf{C}_v \tag{9}$$

where: $\mathbf{P}_l$ is the vector of lateral inertial loads applied at the n_s stories of the structure; $\mathbf{C}_v$ is the vector of lateral inertia load distribution factors $C_{v,s}$ (s =1,…, n_s), which is determined from, [5],

$$C_{v,s} = \frac{P_s}{V_b} = \frac{G_s H_s^{\lambda}}{\sum_{t=1}^{n_s} G_t H_t^{\lambda}} \tag{10}$$

where: P_s is the lateral inertial load applied at story level s; G_s and G_t are the portions of the building seismic weight at story levels s and t, respectively; H_s and H_t are the vertical distances (or heights) from the base of the building to story levels s and t, respectively; n_s is the number of stories; and λ is an exponent whose value depends on the fundamental period of the structure.

The elastic fundamental period of the structure T is found as, [4],

$$T = 2\pi \left[\frac{\sum_{s=1}^{n_s} \left(m_s v_s^2 \right)}{\sum_{s=1}^{n_s} \left(V_1 C_{v,s} v_s \right)} \right]^{1/2} \tag{11}$$

where: m_s is the seismic mass of story s; V_1 is a base shear force taken to be sufficiently small to ensure that the resulting lateral displacement v_s of story level s corresponds to elastic behaviour of the structure.

The overall vector **P** of nodal loads accounting for both lateral inertial and gravity loading is given by,

$$\mathbf{P} = \mathbf{D}\,\mathbf{P}_l + \mathbf{P}_g \tag{12}$$

where **D** is a Boolean matrix, and $\mathbf{P}_g$ is the vector of nodal gravity loads for the structure (see examples of **P**, **D,** $\mathbf{P}_l$, and $\mathbf{P}_g$ in Appendix).

The pushover analysis use centerline dimensions to model all frame members. Rigid beam-to-column connections are assumed. Panel zone deformation is neglected. More detailed descriptions on the pushover analysis were given by Hasan et al. [7] and Gong [21].

3. OPTIMAL DESIGN PROBLEM FORMULATION

3.1 Objective Criteria

Two design objectives concerning structural cost and uniform ductility demand are identified for this study.

Minimum structural cost is perhaps the most favorable design objective and is commonly adopted by many optimization problems. Some attempts (e.g.,Wen and Kang [22]) have been made to develop a general building cost function. Unfortunately, a complete description of the real cost of a building before its construction is often nearly impossible because many factors that affect the cost are unpredictable and not precisely defined. As the mathematical formulation of a meaningful cost function in a truly broad context is virtually impossible to achieve for a structural framing system considered in isolation, as herein, the cost of the members of the structure is alone taken to define the cost objective function for this study, while structural fabrication and erection costs are implicitly considered in the design process through a member grouping technique, illustrated by the design example in Section 6. Assuming that the cost of a member is proportional to its material weight, the least-cost design can be interpreted as the least-weight design of the structure, and the cost objective function f_1 (also called the weight objective) to be minimized is formulated as:

$$f_1(\mathbf{x}) = \frac{1}{W_{\max}} \sum_{j=1}^{n_e} \rho L_j A_j \tag{13}$$

where: **x** is the generic representation of the vector of design variables; ρ is the material mass density; n_e is the number of members; L_j and A_j are the length and cross-section area of the jth member, respectively. The function f_1 is normalized by the maximum possible weight of the frame W_{max}, which is calculated as $W_{max}=\sum \rho L_j A_j^U$, where A_j^U is the upper-bound cross section area for member j (j=1,2,...n) and taken from AISC Manual [23] for this study. The normalization facilitates the numerical realization of the design formulation since the value of f_1 always varies in the range $0 \le f_1 \le 1$ whatever size the structure is and whatever unit is used for computing the structural weight. Furthermore, the magnitude of f_1 value is at the same order as that of objective function f_2, which is introduced in the following.

It has been observed in many collapsed structures that deformation concentration took place at a soft (or weak) story under severe earthquake loading, which directly led to building failure. To avoid the weak or soft story failure, it is necessary to design the structure such that the ductility demands in all the stories are similar. In other words, a uniform heightwise ductility demand is a desirable objective for seismic design [4]. To this end, since a building exhibiting a uniform plastic interstory drift distribution experiences minimum plastic deformation concentration, the uniform ductility design objective can be interpreted as pursuing a uniform heightwise plastic interstory

drift distribution. Therefore, this design objective can be formulated as to minimize the following function f_2 as, [14]:

$$f_2(\mathbf{x}) = \left[\frac{1}{n_s} \sum_{s=1}^{n_s-1} \left(\frac{v_s(\mathbf{x})/H_s}{\Delta(\mathbf{x})/H} - 1 \right)^2 \right]^{1/2} \tag{14}$$

where H_s and H are the distances from the building ground level to story s and the roof, respectively, while $v_s(\mathbf{x})$ and $\Delta(\mathbf{x})$ are the lateral plastic deflections of story s and the building roof under the considered earthquake hazard, respectively. In effect, f_2 defines the coefficient of variation of the story drift distribution, since v_s/H_s and Δ/H represent the plastic story drift ratio and the building mean drift ratio, respectively. By definition, the value of $f_2(\mathbf{x})$ is not less than zero, and only for the extreme case of a perfectly uniform interstory drift distribution is $f_2(\mathbf{x})=0$.

3.2 Design Variables

The cross section sizes of the members are taken to be design variables for this study. Four cross-sectional properties, i.e., the area A, moment of inertia I, elastic modulus S (associated with first yield) and plastic modulus Z (associated with full plasticity) are required in pushover analysis. For a specified type and nominal depth of commercially available standard steel sections, these four properties can be related together through functional relationships which are expressed as:

$$I = C_1 A^2 + C_2 A + C_3 \tag{15}$$

$$S = C_4 A + C_5 \tag{16}$$

$$Z = f_s S \tag{17}$$

$$Z = C_6 (1/A)^{C7} \tag{18}$$

where C_1 to C_7 are constants determined by regression analysis [21]. For examples, the values of C_1 to C_7 for some commercial W sections of specified nominal depths [23] are listed in Table 1. Having such relationships, the cross section area A can be taken as the only design sizing variable, thereby reducing the number of design variables significantly. Equations (15) to (17) play an important role in the design automation since pushover analysis results are very sensitive to the sectional properties I, S and Z, which therefore need to be estimated as accurately as possible during the design process. Equation (18) is used to formulate strong-column weak-beam constraints in terms of reciprocal variables (see Subsection 3.4).

Table 1. Section Properties Relationships

Section Type	$I = C_1 A^2 + C_2 A + C_3$			$S = C_4 A + C_5$		$Z = C_6 (1/A)^{C7}$	
	C_1	C_2	C_3	C_4	C_5	C_6	C_7
W14	0.14	22922	–25781536	5.95	–25.64	82.39	–1.05
W30	0.12	115380	–536216897	11.42	–55.77	77.76	–1.12

Note: unit of millimeter is used for all properties.

3.3 Design Constraints

According to the roles they play in determining design variables, design constraints can be classified as being primary or secondary. Those that play major roles in the design selection are referred to as primary constraints, while those that are not expected to significantly participate in the design selection are labeled as secondary constraints. For this study, the following three types of constraints are considered:

(1) Drift constraints, which are primary design constraints for steel moment frames in high seismic zones [24].
(2) Strong column/weak-beam constraints, which are mandatory requirement for special moment frames [25].
(3) Side constraints. The lower and upper limits imposed on the values of the design variables.

The member strength requirements are secondary for the seismic design in high seismic zones. Foutch and Yun [24] concluded that the drift limitation always governs in high seismic zones for new steel moment frame buildings. For the sake of simplicity, the member strength requirements are not included in the design formulation in this study. However, they can be easily incorporated into the side constraints if necessary (Chan et al. [26]).

3.3.1 Drift constraints

Moderate drift or lateral deflection of a building may cause human discomfort, and minor damage of nonstructural components, such as cracking of partitions or cladding and the leakage of pipes. Large inelastic drift due to an extreme earthquake can cause the failure of mechanical, electrical and plumbing systems, or cause suspended ceilings and equipment to fall, thereby posing threats to human life. Thus, it is essential to control the drift of building frameworks under seismic loading.

There are two kinds of lateral drifts to be considered in design practice. One is the overall building drift (roof drift). The other is the interstory drift, defined as the drift difference between two adjacent floors. The overall building drift represents the average lateral translation. For this study, a roof drift constraint is imposed in the design formulation, i.e.,

$$\Delta(\mathbf{x}) \le \bar{\Delta} \tag{19}$$

where $\bar{\Delta}$ is allowable roof drift, which is taken as the target displacement under the considered earthquake hazard. A target displacement is the maximum roof lateral deflection likely to be experienced by the structure during the design earthquake.

Interstory drift can be related to the plastic rotation demand imposed on individual beam-column connection assemblies, and is therefore an excellent predictor of the performance of beams, columns and connections [27]. Design standards normally requires limitation on interstory drift, which are expressed as,

$$\delta_s(\mathbf{x}) \le \bar{\delta} \quad (s = 1, \cdots n_s) \tag{20}$$

where: δ_s is the interstory drift of story s (i.e., $\delta_s = v_s - v_{s\text{-}1}$, the difference between the drift v_s at story s and the drift $v_{s\text{-}1}$ at story s-1); $\bar{\delta}$ is the allowable interstory drift. δ/h is called interstory drift ratio, where h is the height of the corresponding story. The allowable interstory drift $\bar{\delta}$ is determined accounting for the desired structural performance and interstory drift capacity [27].

3.3.2 Strong-column weak-beam constraints

In earthquake engineering, one of the design goals is to provide the structure with good energy dissipation capacity. In this regard, the 'Strong-Column Weak-Beam' (SC/WB) concept is introduced in seismic provisions as a means to help meet this objective for moment frames. The SC/WB concept is implemented through the following constraint applied at beam-to-column connections, [25]:

$$r_{cb} = \frac{\sum M^*_{pc}}{\sum M^*_{pb}} > 1.0 \tag{21}$$

where: r_{cb} is the so-called column-beam moment ratio; $\sum M_{pc}{}^*$ is the sum of the moment capacities in the column above and below the joint, calculated as $\sum M_{pc}{}^* = \sum[(Z)(\sigma_y - N/A)]$ (where N is the axial compressive force for the column and σ_y is the design yield strength.); $\sum M_{pb}{}^*$ is the sum of moment capacities in the beams at the joint, calculated as $\sum M_{pb}{}^* = \sum[1.1(Z)(\sigma_{ye}) + M_v]$ (where the factor of 1.1 is introduced to recognize the potential over-strength of beams due to other considerations; M_v is the additional moment due to shear amplification from the location of the plastic hinge to the column centerline. M_v is zero for this study since centerline dimensions are used in the structural model and plastic hinges are assumed to occur at the ends of members); and subscripts *b* and *c* refer to beams and columns at the connection under consideration.

The SC/WB provision is mandatory only for special moment frames in AISC Seismic Provisions [25]. It is noted that axial compressive force in columns is taken into account in calculating $\sum M_{pc}{}^*$ while axial tensile force is ignored when using Eq. (21). No reason is given in its companion commentary for this discrimination between tensile and compressive forces [25].

3.4 Design Formulation

Generally speaking, it is desirable to use commercially available standard sections to proportion steel frameworks. To this end, the design process is carried out in two phases. Phase I treats the design as a continuous variable design problem. Phase II utilizes a dynamic rounding-off strategy to find the discrete commercial section for each design variable based on the phase I results. Each phase further includes two stages. The objective of Stage One is to search for a least-weight design, while the objective of Stage Two is to search for a uniform ductility design. A detailed step-by-step description of design procedure is given in Section 5.

From the foregoing, the optimization model is formulated as:

$$\text{Minimize} \quad f_1(\mathbf{x}) = \frac{1}{W_{\max}} \sum_{j=1}^{n_e} \rho L_j A_j \quad \text{at Stage One} \tag{22}$$

or

$$\text{Minimize} \quad f_2(\mathbf{x}) = \left[\frac{1}{n_s} \sum_{s=1}^{n_s-1} \left(\frac{v(\mathbf{x})/H_s}{\Delta(\mathbf{x})/H} - 1 \right)^2 \right]^{1/2} \quad \text{at Stage Two} \tag{23}$$

$$\text{Subject to:} \quad \Delta(\mathbf{x}) \le \overline{\Delta} \tag{24}$$

$$\delta_s(\mathbf{x}) \le \bar{\delta} \quad (s = 1, \cdots n_s) \tag{25}$$

$$A_j^L \le A_j \le A_j^U \quad (j = 1, 2, \cdots, n_e) \tag{26}$$

and SC/WB constraints for special moment frames:

$$-\sum_c \left[Z \cdot \left(\sigma_y - \frac{N}{A} \right) \right]_c + \sum_b \left(1.1 \cdot Z \cdot \sigma_{ye} \right)_b \le 0 \tag{27}$$

Design constraints, Eqs. (24) to (27), are the same for both Stages One and Two. Equations (26) are side constraints, where sizing limitations are taken as the lower and upper bounds A^L and A^U on the cross-sectional areas A of commercially available sections (see design example in Section 6). Equation (27) for the constraints, which are imposed to the specified joints, is derived from Eq. (21), where subscripts *c* and *b* refer to column and beam at the specified joint, respectively.

The idea of the two-stage design strategy is inspired by the finding that a uniform ductility design can be obtained with a structural weight being only slightly greater than that of a pure minimum-weight design in a pilot study conducted by the author [21]. In Stage One, a minimum-weight design is obtained subject to drift and side constraints (and SC/WB constraints for special moment frames). In Stage Two, an optimal design with an improved ductility distribution over the minimum-weight design is obtained. This two-stage strategy eliminates the necessity of combining the two design objectives into one (a practice often involves arduous numerical efforts in determining the combination factors for the multi-objective optimization [14, 21]).

The dynamic rounding-off strategy (also called pseudo-discrete section selection strategy by Chan *et al.* [26]) employed in Phase II to find discrete sections is a modification of the simple rounding-up method that rounds up all section sizes found from the continuous optimization solution to their nearest available discrete section sizes. While the simple rounding-up method is direct and easy to implement, it sometimes results in a significant stiffness redistribution for the structure that can make the design solution infeasible [28]. Also, it overlooks the fact that it is often unnecessary to increase all the variables to their nearest upper discrete values as some of them could be just as well decreased to their nearest lower discrete values. Instead of assigning all design variables to their nearest upper discrete values at one time, the dynamic rounding-off method rounds up only one or a few variables at a time. Then, the selected variable(s) are fixed at their assigned discrete value and the design is optimized again for the reduced set of remaining variables. This process is repeated until all variables have been selected and assigned discrete values.

To enable computer solution of the design optimization problem, it is necessary to use an approximation technique to formulate Eqs. (23) to (25) explicitly in terms of design variables. High quality approximations can be obtained by adopting the reciprocal variables, [29],

$$x_j = \frac{1}{A_j} \tag{28}$$

and then employing first-order Taylor series to reformulate Eqs. (22) to (27) as the explicit design problem,

$$\text{Minimize} \quad f_1(\mathbf{x}) = \frac{1}{W_{\max}} \sum_{j=1}^{n_e} \frac{\rho L_j}{x_j} \quad \text{at Stage One} \tag{29}$$

or

$$\text{Minimize} \quad f_2(\mathbf{x}) = [f_2(\mathbf{x})]^0 + \sum_{j=1}^{n_e} \left[\frac{df_2(\mathbf{x})}{dx_j} \right]^0 \left(x_j - x_j^0 \right) \text{ at Stage Two} \tag{30}$$

$$\text{Subject to:} \quad [\Delta(\mathbf{x})]^0 + \sum_{j=1}^{n_e} \left[\frac{d\Delta(\mathbf{x})}{dx_j} \right]^0 \left(x_j - x_j^0 \right) \le \bar{\Delta} \tag{31}$$

$$[\delta_s(\mathbf{x})]^0 + \sum_{j=1}^{n_e} \left[\frac{d\delta_s(\mathbf{x})}{dx_j} \right]^0 \left(x_j - x_j^0 \right) \le \bar{\delta} \quad (s = 1, \cdots n_s) \tag{32}$$

$$x_j^L \le x_j \le x_j^U \qquad (j = 1, 2, \cdots, n_e) \tag{33}$$

and SC/WB constraints for special moment frames:

$$\sum_c c_c x_c + \sum_b c_b x_b - g_{cb}^U \le 0 \tag{34}$$

where: superscript ' ^{0} ' represents values for the current design; x_j^L and x_j^U are lower and upper bounds on the reciprocal area x_j, respectively, where $x_j^L = 1/A_j^U$ and $x_j^U = 1/A_j^L$; df_2/dx_j, $d\Delta/dx_j$, and $d\delta/dx_j$ are the sensitivities of objective function f_2, roof drift Δ and interstory drift δ with respect to the design variable x_j, respectively. The formulations of these sensitivities are presented in Section 4.

The SC/WB equation of constraints, Eq. (34), is derived as described in the following. Firstly, Z is approximated by a first-order Taylor series formulated at the current design point x^0 by applying Eq. (18), i.e.,

$$Z = Z^0 + \left(\frac{dZ}{dx} \right)^0 \left(x - x^0 \right) \tag{35}$$

where

$$\frac{dZ}{dx} = C_6 C_7 \left(\frac{1}{A} \right)^{C_7 - 1} = C_6 C_7 x^{C_7 - 1} \tag{36}$$

Equation (34) is obtained by substituting Eq. (35) into Eq. (27) and then by defining the following coefficients:

$$c_c = -\left(\frac{dZ}{dx} \right)_c^0 \left(\sigma_y - \frac{N}{A} \right)_c \tag{37}$$

$$c_b = 1.1 \left(\frac{dZ}{dx} \right)_b^0 \left(\sigma_{ye} \right)_b \tag{38}$$

$$g_{cb}^{U} = \sum_{c}\left[Z^0 - \left(\frac{dZ}{dx}\right)^0 x^0 \right]_c \left(\sigma_y - \frac{N}{A} \right)_c - \sum_{b} 1.1 \left[Z^0 - \left(\frac{dZ}{dx}\right)^0 x^0 \right]_b \left(\sigma_{ye} \right)_b \tag{39}$$

The optimization model Eqs. (29) to (34) is solved iteratively by using numerical optimization techniques. Each iteration begins with a pushover analysis of the current design to compute the values of objective function (i.e., f_2^0 in Eq. (30)) and constraints (i.e., Δ^0 and δ_s^0 in Eqs. (31) and (32)) along with sensitivities (i.e., $(df_2/dx_j)^0$, $(d\Delta/dx_j)^0$ and $(d\delta_s/dx_j)^0$ in Eqs. (30) to (32)). Then a minimization algorithm called Dual method [30] is employed to solve Eqs. (29) to (34) for an improved design, which is further taken as the current design for the next iteration.

4. SENSITIVITY ANALYSIS

Gong et al. [31, 32] derived sensitivity analysis formulations for the pushover analysis procedure described in Section 2. For the completeness of this paper, the sensitivity formulations are given briefly in the following.

The equilibrium equations for a pushover analysis can be stated as,

$$\mathbf{F}(\mathbf{u}, \mathbf{A}) = \mathbf{P}(\mathbf{A}) \tag{40}$$

where: $\mathbf{F}(\mathbf{u}, \mathbf{A})$ is the overall internal nodal force vector; $\mathbf{P}(\mathbf{A})$ is the overall externally applied nodal load vector in Eq. (12); $\mathbf{u}$ is the vector of nodal displacements; $\mathbf{A}$ is the vector of design variables which are taken as the cross sectional areas of the members.

Differentiating Eq. (40) with respect to design variable A_j gives

$$\mathbf{K}^t \frac{d\mathbf{u}}{dA_j} = \frac{d\mathbf{P}}{dA_j} - \frac{\partial \mathbf{F}}{\partial A_j} \tag{41}$$

where $\mathbf{K}^t = \partial\mathbf{F}/\partial\mathbf{u}$ is the global tangential stiffness matrix. $d\mathbf{P}/dA_j$ is the sensitivity of the nodal load vector with respect to design variable A_j. For this study, $d\mathbf{P}/dA_j$ reflects the influence of structural modifications on earthquake loading.

Consider a particular displacement μ_l for a given framework, which is related to the overall vector of nodal displacements $\mathbf{u}$ as,

$$\mu_l = \mathbf{b}_l^T \mathbf{u} \tag{42}$$

where $\mathbf{b}_l$ is a Boolean vector (consisting of 0 and 1) that depends on the nature of displacement μ_l. For instance, if $\mu_l = v_1$ is the lateral drift of a story, the vector $\mathbf{b}_l$ is obtained by setting the component entries corresponding to degrees of freedom v_1 to unity while setting the rest of the entries to zero; namely, $\mathbf{b}_l^T = \{1, 0, 0, \ldots, 0\}$ assuming that v_1 corresponds to degree of freedom 1.

The sensitivity of displacement μ_l with respect to changes in design variable A_j is then found as, from Eqs. (42) and (41),

$$\frac{d\mu_l}{dA_j} = \mathbf{b}_l^T \frac{d\mathbf{u}}{dA_j} = \mathbf{U}_l^T \left[\frac{d\mathbf{P}}{dA_j} - \frac{\partial \mathbf{F}}{\partial A_j} \right] \tag{43}$$

where $\mathbf{U}_l^T = \mathbf{b}_l^T \mathbf{K}^{t\text{-}1}$ or $\mathbf{U}_l = \mathbf{K}^{t-1} \mathbf{b}_l$.

The major effort in nonlinear sensitivity analysis is the evaluation of the partial derivatives of internal nodal forces, i.e., the term $\partial \mathbf{F} / \partial A_j$ in Eq. (43). Since the pushover analysis uses the incremental-load method, the vector of internal nodal forces is equal to

$$\mathbf{F} = \sum_m \Delta \mathbf{F}^{(m)} \tag{44}$$

where m is the load-step index and $\Delta \mathbf{F}^{(m)}$ represents the increment of internal nodal forces at load step m. Differentiating Eq. (44) with respect to design variable A_j gives,

$$\frac{\partial \mathbf{F}}{\partial A_j} = \sum_m \frac{\partial \Delta \mathbf{F}^{(m)}}{\partial A_j} = \sum_m \frac{\partial \left[\sum_{k=1}^{n_e} \left(\mathbf{T}_k^T \mathbf{K}_k^{(m)} \mathbf{T}_k \cdot \Delta \mathbf{u}^{(m)} \right) \right]}{\partial A_j} = \sum_m \left[\sum_{k=1}^{n_e} \left(\mathbf{T}_k^T \frac{\partial \mathbf{K}_k^{(m)}}{\partial A_j} \mathbf{T}_k \Delta \mathbf{u}^{(m)} \right) \right] \tag{45}$$

where: $\mathbf{T}_k$ is the direction-cosine matrix for member k; $\Delta \mathbf{u}$ is the vector of incremental nodal displacements; $\mathbf{K}_k$ is the stiffness matrix for element k; and from Eq. (1),

$$\frac{\partial \mathbf{K}_k^{(m)}}{\partial A_j} = \frac{\partial \mathbf{S}_k}{\partial A_j} \mathbf{C}_{sk}^{(m)} + \mathbf{S}_k \frac{\partial \mathbf{C}_{sk}^{(m)}}{\partial A_j} + \frac{\partial \mathbf{G}_k^{(m)}}{\partial A_j} \mathbf{C}_{gk}^{(m)} + \mathbf{G}_k^{(m)} \frac{\partial \mathbf{C}_{gk}^{(m)}}{\partial A_j} \tag{46}$$

where: $\partial \mathbf{C}_{sk} / \partial A_j$ and $\partial \mathbf{C}_{gk} / \partial A_j$ are the derivatives of correction matrices $\mathbf{C}_{sk}$ and $\mathbf{C}_{gk}$, respectively [32]; $\partial \mathbf{S}_k / \partial A_j$ and $\partial \mathbf{G}_k / \partial A_j$ are the derivative of elastic stiffness matrix $\mathbf{S}_k$ and geometric stiffness matrix $\mathbf{G}_k$, respectively.

By assuming $\partial \mathbf{K}_k^{(m)} / \partial A_j = 0$ if $k \neq j$ [32] and expanding Eq. (46) in terms of plasticity factors, the sensitivity of displacement μ_l is then derived from Eqs. (43) and (44) as

$$\frac{d\mu_l}{dA_j} = \mathbf{U}_l^T \frac{d\mathbf{P}}{dA_j} - \mathbf{U}_l^T \sum_m \left\{ \mathbf{T}_j^T \left[\frac{\mathbf{S}_j \mathbf{C}_{sj}^{(m)}}{A_j} + \sum_{n=1}^{2} \left(\mathbf{S}_j \frac{\partial \mathbf{C}_{sj}^{(m)}}{\partial p_{jn}^{(m-1)}} + \mathbf{G}_j^{(m)} \frac{\partial \mathbf{C}_{gj}^{(m)}}{\partial p_{jn}^{(m-1)}} \right) \bullet \right.$$
$$\left. \left(\frac{\left(p_{jn}^{(m-1)} - 1 \right) p_{jn}^{(m-1)}}{A_j} + \frac{\left(1 - p_{jn}^{(m-1)} \right)^2 L_j}{3EI_j} \frac{\partial R_{jn}^{p(m-1)}}{\partial A_j} \right) \right] \mathbf{T}_j \Delta \mathbf{u}^{(m)} \right\} \tag{47}$$

where: p_{jn} is the plasticity-factor in Eq. (2) for element j at end n (n=1 or 2); $\partial R_{jn}^P / \partial A_j$ is the derivative of rotational stiffness of the plastic hinge for element j at end n; and supercript (m-1) is load step index. See [32] for detailed derivation of Eq. (47).

Equation (47) reduces to the well-known static elastic displacement sensitivity formulation when p_{jn}=1, m=1, and $d\mathbf{P}/dA_j$=0; i.e.,

$$\frac{d\mu_l}{dA_j} = -\frac{1}{A_j}\mathbf{U}_l^T\left(\mathbf{T}_j^T\mathbf{K}_j\mathbf{T}_j\right)\mathbf{u} \tag{48}$$

The sensitivity of overall nodal load vector, $d\mathbf{P}/dA_j$ in Eq. (47), is found from Eq. (12) as,

$$\frac{d\mathbf{P}}{dA_j} = \mathbf{D}\frac{d\mathbf{P}_l}{dA_j} + \frac{d\mathbf{P}_g}{dA_j} = \mathbf{D}\frac{d\mathbf{P}_l}{dA_j} \tag{49}$$

where $d\mathbf{P}_g/dA_j$=0 since the $\mathbf{P}_g$ load vector is constant for pushover analysis, and $d\mathbf{P}_l/dA_j$ is found by differentiating Eq. (9) with respect to the design variable A_j, to get,

$$\frac{d\mathbf{P}_l}{dA_j} = \frac{dV_b}{dA_j}\mathbf{C}_v \tag{50}$$

where dV_b/dA_j is the sensitivity of the design base shear which, from Eqs. (7) and (8), is found as,

$$\frac{dV_b}{dA_j} = \frac{W}{g}\frac{\partial S_a}{\partial T}\frac{dT}{dA_j} = \begin{cases} 0 & T \le T_0 \\ -\dfrac{W}{g}\dfrac{S_1}{T^2}\dfrac{dT}{dA_j} & T > T_0 \end{cases} \tag{51}$$

in which, from Eq. (11),

$$\frac{dT}{dA_j} = \sum_{s=1}^{n_s}\frac{\partial T}{\partial v_s}\frac{dv_s}{dA_j} = \sum_{s=1}^{n_s}\frac{2\pi^2}{T\sum_{t=1}^{n_s}\left(V_1 C_{v,t} v_t\right)}\left(2 m_s v_s - \frac{T^2 V_1 C_{v,s}}{4\pi^2}\right)\frac{dv_s}{dA_j} \tag{52}$$

In Eq. (52): $C_{v,t}$ is the inertia load distribution factor at story level t (see Eq. (10)); v_t is story drift under the action of base shear V_1 at story level t; and dv_s/dA_j is the static elastic sensitivity of story drift v_s, since V_1 is a constant, and is found from Eq. (48).

Then, the sensitivity of objective function f_2 is found as:

$$\frac{df_2}{dA_j} = \sum_{s=1}^{n_s-1}\left(\frac{\partial f_2}{\partial v_s}\frac{dv_s}{dA_j}\right) + \frac{\partial f_2}{\partial \Delta}\frac{d\Delta}{dA_j} \tag{53}$$

where:

$$\frac{\partial f_2}{\partial v_s} = \frac{1/H_s}{n_s f_2(\Delta/H)}\left(\frac{v_s/H_s}{\Delta/H} - 1\right) \tag{54}$$

and

$$\frac{\partial f_2}{\partial \Delta} = \frac{1}{n_s f_2}\sum_{s=1}^{n_s-1}\left(\frac{v_s/H_s}{\Delta/H} - 1\right)\left(-\frac{v_s/H_s}{\Delta^2/H}\right) \tag{55}$$

Finally, the sensitivity of a general structural response R_s with respect to reciprocal variable x_j can be restored from

$$\frac{dR_s}{dx_j} = \frac{dR_s}{dA_j}\frac{dA_j}{dx_j} = -A_j^2\frac{dR_s}{dA_j} \tag{56}$$

where a general structural response R_s can be drift v_s or Δ, or period T, or design base shear V_b, or objective function f_2, etc.

5. OPTIMAL DESIGN PROCEDURE

In summary, the overall design procedure is described step-by-step in the following:

(1) Input geometry of the structure, such as bay size and story height, etc. Input design spectrum (Eq. (8)), constraint limits (i.e., $\overline{\Delta}$ and $\overline{\delta}$), seismic weights (W and G_s), and the number of design variables n_e. Set design iteration index i=0.

(2) Assume initial member sizes $\mathbf{x}_i$. Recover section properties from the section databank (AISC Manual [23] is adopted for this study).

(3) Set design phase index PI=1 (i.e., continuous optimization)

(3.1) Stage One

- (3.1.1) Set design iteration index $i=i+1$. Calculate f_1 value for current design.
- (3.1.2) Apply base shear V_1 to the structure with no gravitational loads, and conduct elastic analysis to compute the period T by Eq. (11), the acceleration response S_a by Eq. (8), and the design base shear V_b by Eq. (7).
- (3.1.3) Perform pushover analysis to evaluate the structural responses under design base shear V_b.
- (3.1.4) Calculate sensitivities $d\Delta/dx_j$ and $d\delta_s/dx_j$ using Eq. (47).
- (3.1.5) Formulate design optimization problem, Eqs. (29), (31) to (34).
- (3.1.6) Apply the Dual method [21] to search for an improved design, $\mathbf{x}_{i+1}$.
- (3.1.7) Check the convergence criteria for the design point $\mathbf{x}_{i+1}$. If $\mathbf{x}_{i+1}$ is not convergent, update section properties according to Eqs. (15) to (18), and go back to step 3.1.1. If $\mathbf{x}_{i+1}$ is found to be convergent (e.g., the difference of structural weight between two consecutive cycles is less than 0.3%), terminate Stage One and proceed to Stage Two at step 3.2.

(3.2) Stage Two

- (3.2.1) Repeat Step 3.1.1 to 3.1.3.
- (3.2.2) Calculate f_2 value for current design. Check the convergence criteria (e.g., the improvement of f_2 value for three consecutive cycles is less than 1%). If $\mathbf{x}_i$ is not convergent, go to step 3.2.3. If $\mathbf{x}_{i+1}$ is found to be convergent, terminate Stage Two and proceed to Phase II at step 4.
- (3.2.3) Calculate sensitivities df_2/dx_j, $d\Delta/dx_j$ and $d\delta_s/dx_j$.
- (3.2.4) Formulate design optimization problem, Eqs. (30) to (34).
- (3.2.5) Apply the Dual method to search for an improved design, $\mathbf{x}_{i+1}$.
- (3.2.6) Go to step 3.2.1

(4) Set design phase index PI=2 (i.e., discrete optimization).

(4.1) Select one or a few variables to be assigned to their nearest upper discrete sizes, and

compute the number of design variables remaining to be assigned a discrete size.

(4.2) If no design variable remains to be assigned to a discrete size, stop the discrete optimization and go to step 5; otherwise, proceed to step 4.3.

(4.3) Update sectional properties for discrete-size sections (i.e., the design variables that have already been assigned a discrete size) from the section databank; update properties of continuous-size sections (i.e., the design variables that remain to be assigned a discrete size) through Eqs. (15) to (18).

(4.4) Perform Stage One and Stage Two optimization (i.e., redo steps 3.1 and 3.2) for the remaining continuous variables.

(4.5) Go to step 4.1.

(5) Perform pushover analysis for the obtained optimal design. Output the results of the design optimization (i.e., optimal discrete section sizes A_j, structural weight f_1, coefficient of variation of the inelastic story drift distribution f_2, member-end plasticity factors p, inter-story drifts δ_s, internal member forces, etc.).

6. DESIGN EXAMPLE

A nine-story rigid moment frame in Figure 4, which was studied by Hasan et al. [7], is adopted as the design example. All five bays are 9.14 m wide (centerline dimensions) and all stories are each 3.96 m high except the first story is 5.5 meters high. The lumped seismic weights for the frame are 4942 kN for the first floor level, 4857 kN for each of the second to eighth floor levels, and 5231 kN for the roof level. Constant gravity loads of 32 kN/m are applied to the beams in the first to eighth floor levels, while 29 kN/m are applied to the roof beams.

The frame consists of 99 members. Through member grouping, the number of design variables is reduced to 19, designated as A_1 to A_{19} in Figure 4. Member grouping is a technique to simulate construction practice in addition to reduce the number of design variables. For example, member grouping is used to mimic tier columns, as shown by column section A_2 in Figure 4. It is a common practice to design all the beams on the same floor level using one cross section, as illustrated by A_{12} in Figure 4. Therefore, this member grouping technique can take cost effective practices into account. On the other hand, member grouping, which can reduce the number of design variables significantly, makes the design optimization algorithm more efficient. Member grouping does not affect all the equations except Eqs. (13) and (56) where a few symbols need to be redefined. For Eq. (13), n_e is redefined as the number of design variables and L_j the sum of the length of each individual member whose cross section is grouped as design variable j. For Eq. (56), dR_s/dx_j is the sum of the sensitivities of R_s with respect to each individual member whose cross section is design variable j.

During the design process, it is required to employ Eqs. (15) to (18) to express section properties I_j, S_j and Z_j in terms of A_j for each of the j=1,2, …, 19 section variables. To this end, it is predetermined that the column design variables A_1 through A_{10} are chosen from among available W14 sections, while beams A_{11} to A_{13}, A_{14} to A_{16}, and A_{17} to A_{19} are chosen from among W36, W30, and W24 sections [23], respectively. While providing considerable *a-priori* knowledge to the design automation algorithm, such predetermination is entirely consistent with conventional design practice where a designer generally knows which type of section and approximate nominal depth is used for a certain type of frame member. For instance, it is well known that W14 sections are commonly used sections for columns, while W24 to W36 sections are often used for beams. If a reasonable section is not able to be chosen from among the predetermined sections to meet the

design requirements, the predetermined sections are upgraded to a larger available nominal depth and the member design process is repeated.

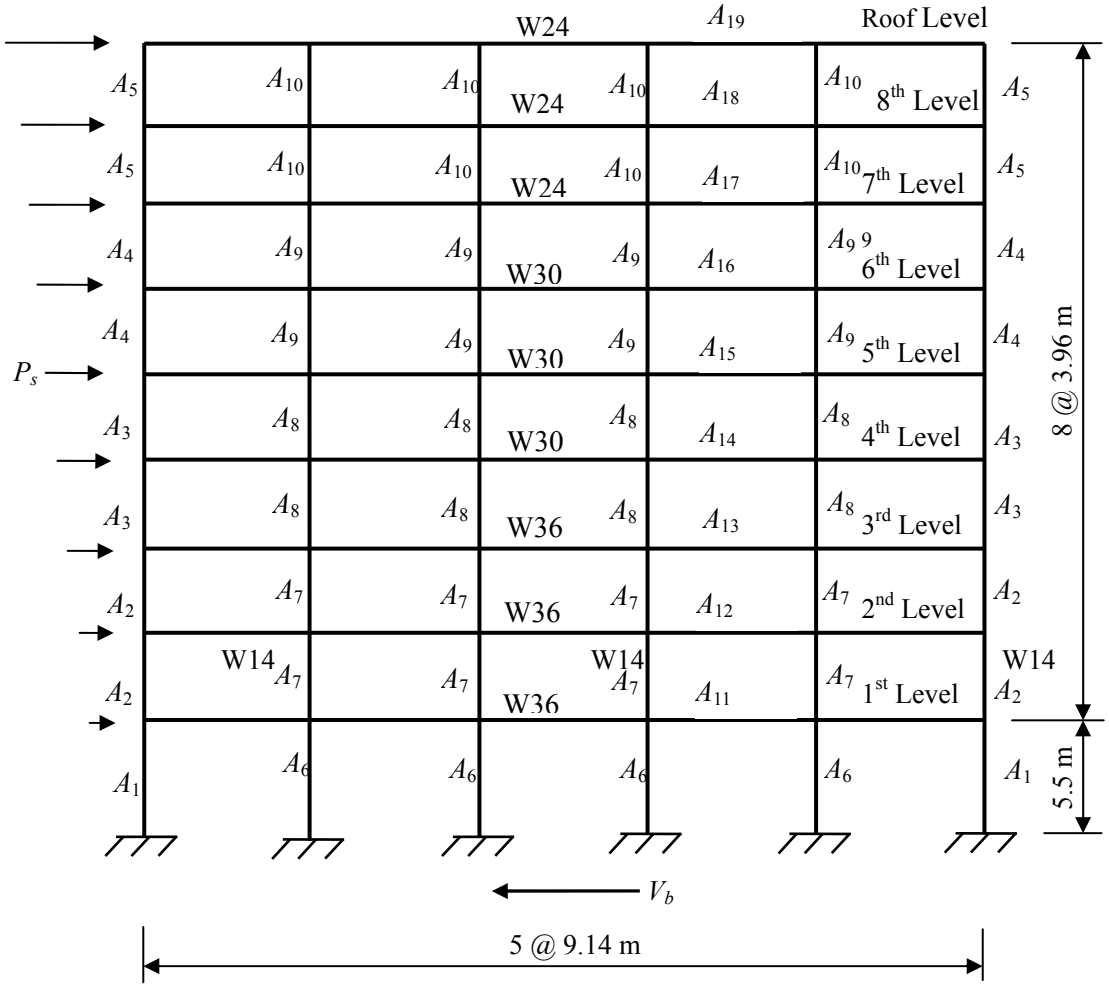

Figure 4. Nine-story Moment Frame

For this study, the initial design point is taken to be defined by the maximum available commercial section sizes for the design variables, i.e., A_1^0 to A_{10}^0 are defined by a W14×808 section, while A_{11}^0 to A_{13}^0, A_{14}^0 to A_{16}^0, and A_{17}^0 to A_{19}^0 are defined by W36×848, W30×477, W24×492 sections, respectively (see Table 2). The maximum weight of the structure is W_{max}=6268 kN, which, in turn, is used to normalize the weight objective function f_1. The lower bounds of design variables are also given in Table 2.

Table 2. Bounds on Member Sizes

Section Shapes	Lower/Upper Section Size	Cross-Section Area A_i (mm^2)
W14	W14×22 W14×808	4190 152900
W24	W24×55 W24×492	10450 92900
W30	W30×90 W30×477	17030 90320
W36	W36×135 W36×848	25610 160640

All the columns use ASTM A572-Grade 50 steel (The nominal yield strength is σ_y=345 MPa and the expected yield strength is $\sigma_{ye} = R_y \sigma_y = 1.1\times345 = 380$ MPa, [25]), while all the beams use A36 steel (σ_y = 248 MPa and σ_{ye} =1.5×248 = 372 MPa).

Design spectrum Eq. (8) is assumed to be as shown in Figure 5. It is expected the obtained design will have $T > T_0$; i.e., the design base shear V_b will change during the design process. The lateral force pattern is determined by Eq. (10) where λ is arbitrarily taken to be 2. The direction of lateral forces is given in Figure 4. The allowable roof drift is taken as the target displacement, which is approximate 0.05 of the building height [6]. Allowable inter-story drift $\bar{\delta}$ is taken to be 0.062h [27], where h is the height of the story under consideration.

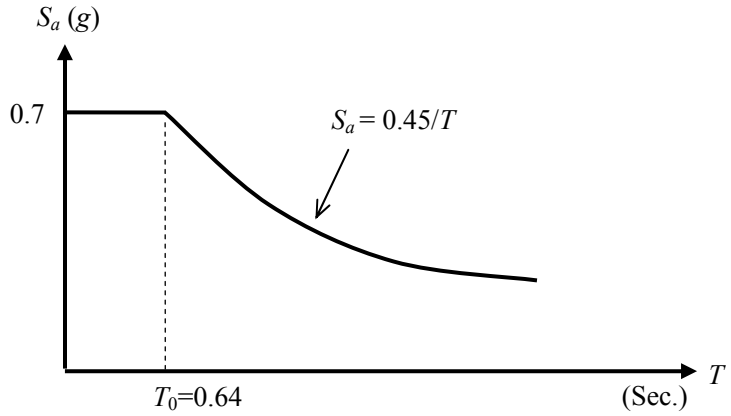

Figure 5. Inelastic Acceleration Response Spectrum

For pushover analysis, each beam member is modeled by four beam elements (i.e., single stress yield condition), while each column is represented by a single beam-column element (i.e., combined stress yield condition). Using one element to model a column will not produce unacceptable error in this study since axial forces in columns of a moment frame are normally far below 40% of the Euler's buckling load [33].

Two runs (i.e., Runs A and B in Table 3) without and with imposing SC/WB constraints to the moment frame are executed to search for optimal solutions (given in Table 3), which are referred to as Designs A and B, respectively. Note that all the commercial standard sections in Table 3 are the type of compact for developing plastic hinges.

Design A, without SC/WB constraints imposed, has a normalized value of the weight objective f_1=0.258 (i.e., the weight of the optimal discrete-section frame is $f_1 \times W_{max}$ = 0.258×6268 = 1616 kN) and a value of f_2=0.03 (i.e., the coefficient of variation of story drift). The elastic period of Design A is 2.26 seconds. The plastic state of Design A under the design base shear V_b=8790 kN is found to be as shown in Figure 6, where ovals represent plastic hinges at member ends and the digit inside ovals represents the percentage of plastification (expressed as 100(1–p), where p is defined by Eq. (2)). As indicated by Figure 6, the first, second, fourth, sixth, and eighth stories have only marginal strength safety against formation of story mechanism, since almost all the columns in these stories have nearly full plastic hinges at both ends. It is noted that these relatively weak stories are where columns splice, i.e., the places where the section size of the columns is reduced abruptly (the first story is seen as a special place where the columns splice). This phenomenon of having relatively weak story in Design A does not conflict with the second design objective, because concentration of interstory drift does not exist based on the pushover analysis results. This phenomenon also illustrates that it is impossible to eliminate story mechanism absolutely under extreme earthquake hazards if SC/WB constraints are not imposed to the design problem.

Table 3. Discrete Design Results of the Nine-story Moment Frame

Design runs	A: No SC/WB	B: With SC/WB
Design variables	Designation A_j (mm^2)	Designation A_j (mm^2)
j= 1	W14×311 58970	W14×342 65160
2	W14×233 44190	W14×283 53740
3	W14×193 36640	W14×283 53740
4	W14×176 33420	W14×233 44190
5	W14×145 27550	W14×211 40000
6	W14×455 86450	W14×500 94830
7	W14×342 65160	W14×398 75480
8	W14×311 58970	W14×370 70320
9	W14×257 48770	W14×311 58970
10	W14×145 27550	W14×283 53740
11	W36×170 32250	W36×170 32250
12	W36×150 28510	W36×150 28510
13	W36×150 28510	W36×135 25610
14	W30×148 28064	W30×173 32770
15	W30×148 28064	W30×148 28064
16	W30×124 23550	W30×108 20450
17	W24×117 22190	W24×103 19550
18	W24×68 12960	W24×94 17870
19	W24×55 10450	W24×62 11740
Weight (kN)	1616	1846

Design B, with SC/WB constraints imposed, has f_1=0.294 (i.e., the weight of the optimal design is $f_1 \times W_{max}$ = 0.294×6268 = 1846 kN) and f_2=0.04. The elastic period of Design B is 2.14 seconds. The plastic state of Design B under V_b=9288 kN is found to be as shown in Figure 7. For this example, SC/WB constraints lead to a heavier optimal design. It is seen from Figure 7 that no soft or weak story exists in Design B. It is noted that the SC/WB constraints cannot prevent individual columns

from yielding even moment ratios r_{cb} at almost all connections are greater than or equal to unity (see Figure 8, where the moment ratios r_{cb} at connections are shown inside ovals. Note that the discrimination between axial tension and compression forces in computing column moment capacity in Eq. (21)). However, it is evident from Figure 7 that beam yielding dominates when the SC/WB constraints are imposed. In reality, a yielding pattern such as that in Figure 7 will most likely eliminate any soft or weak story collapse.

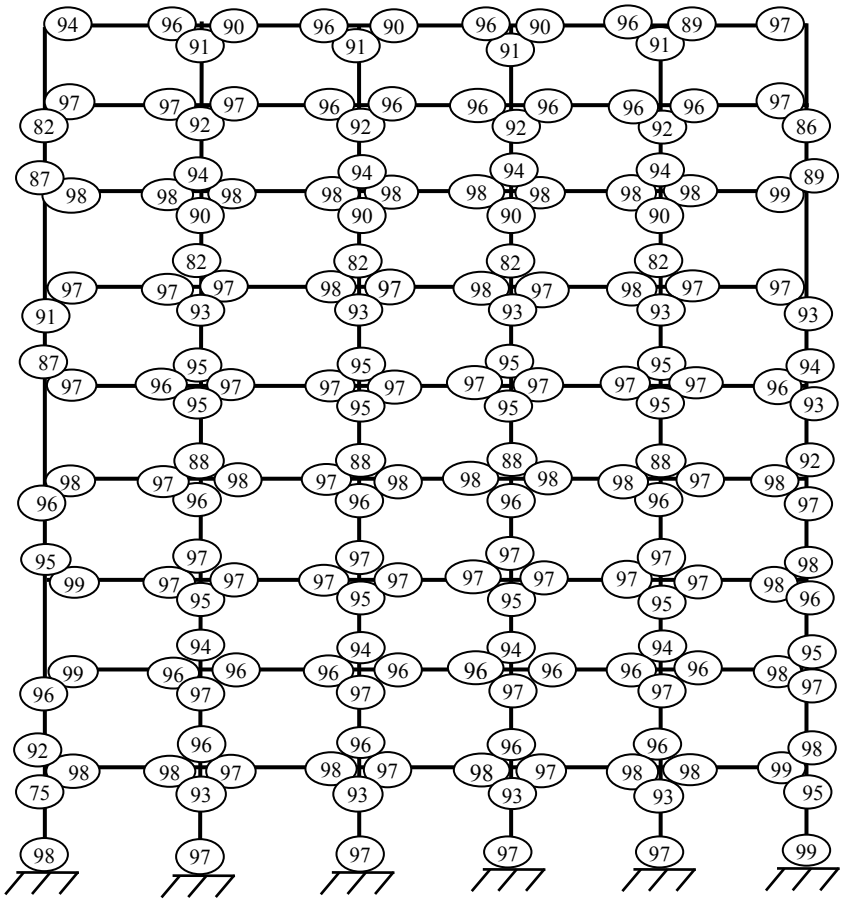

r *r= degree of plastification* = 100 (1-*p*)

Figure 6. Structural Plastification of Design A

The plastic interstory drifts of Designs A and B are given in Table 4. These drift distributions are deemed to be nearly uniform and satisfactory for design. It is generally unlikely to obtain an optimal design with f_2=0 due to the following reasons: 1) the cross sections are discrete variables; 2) the errors in computing sensitivity information are unavoidable [32]; 3) the plastic deflections are extremely sensitive to the change of sectional size (a plastic deflection is usually two orders of magnitude more sensitive than an elastic deflection [31]). For Run A, f_2 =0.03 is the best found by the design algorithm, while for Run B f_2 =0.04 is the optimal. Note that having a smaller f_2 value does not mean Design A is a better solution than Design B. Designs A and B are the optimal solutions under two different sets of constraints (one has SC/WB constraints and the other has not) respectively, thus, it cannot be said that Design A possess a more uniform ductility response than Design B.

Table 4. Interstory Drift Distributions of the Nine-story Moment Frame

Design runs	A: No SC/WB	B: With SC/WB
Story level	Drift ratio	Drift ratio
1	0.040	0.042
2	0.045	0.045
3	0.033	0.047
4	0.054	0.045
5	0.040	0.042
6	0.043	0.055
7	0.037	0.055
8	0.046	0.046
9	0.033	0.033
f_2	0.03	0.04

For member plastification taken as a measure of damage, it is observed from Figures 6 and 7 that damage is somewhat uniformly distributed over all stories of the structures where the frames undergo nearly uniform interstory drift (i.e., as desired, there is no significant concentration of plastic deformation). This phenomenon illustrates the close correlation between the inelastic interstory drift and the structural plastic state. The corresponding pushover capacity curves for Designs A and B are drawn in Figure 9. The global ductility demands can be determined from these curves, which should not exceed the target ductility limit.

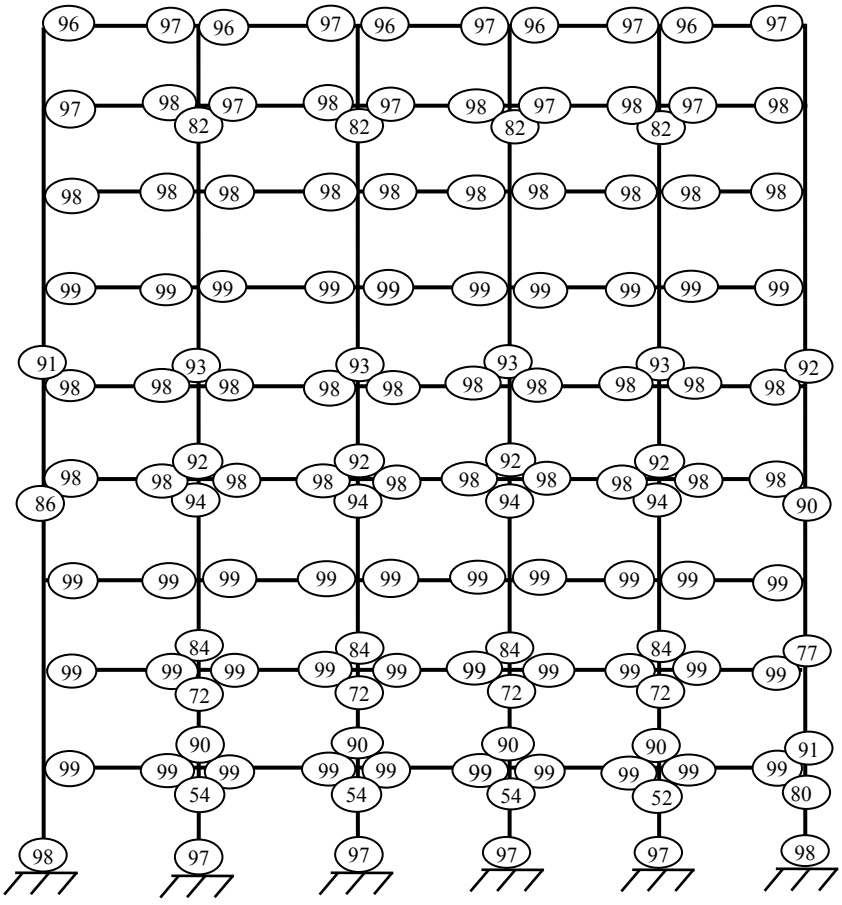

Figure 7. Structural Plastification of Design B

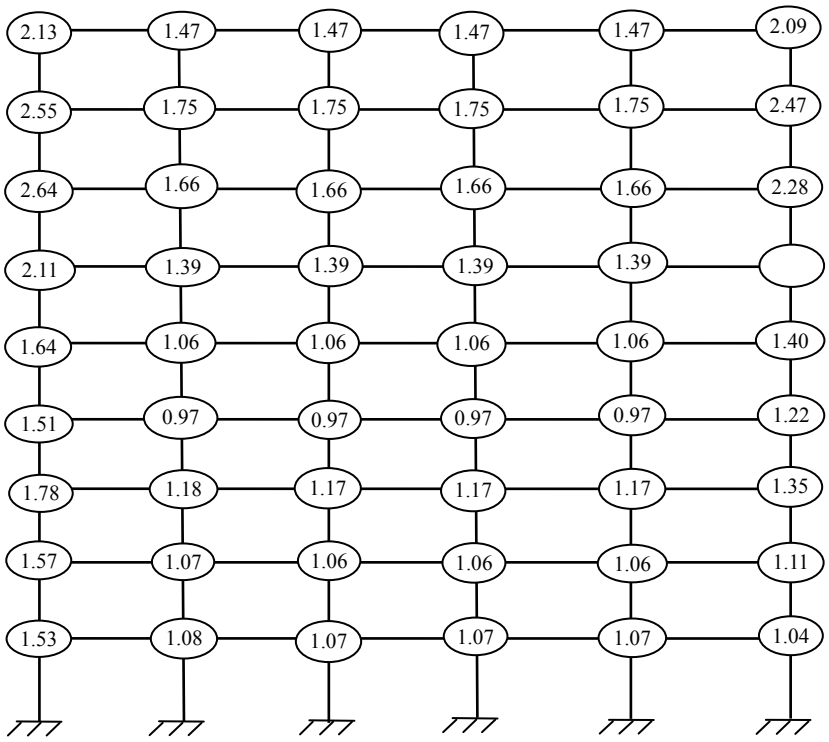

Figure 8. Column-beam Moment Ratios at Connections of Design B

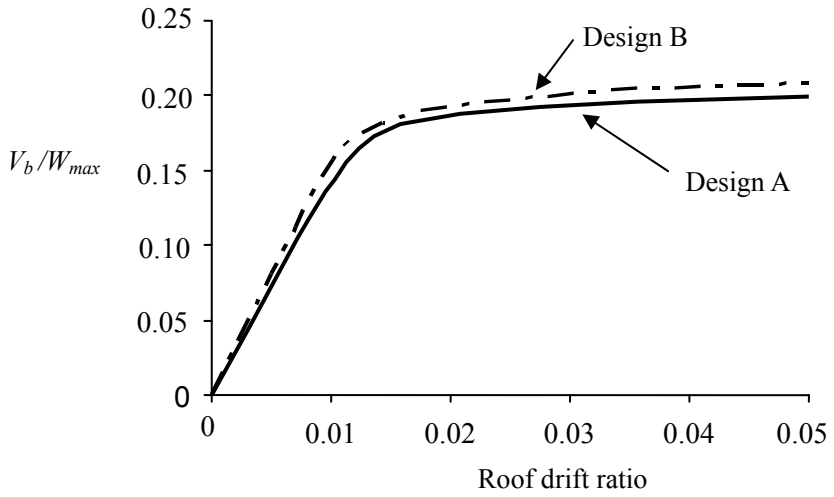

Figure 9. Pushover Capacity Curves for Optimal Designs

Design histories of the normalized structural weights for Runs A and B are illustrated in Figure 10. Phase I (i.e., continuous optimization) ends at iterations 28 and 36 for Runs A and B, respectively. In the early stage of the design history (the first 12 iterations for Run A and the first 15 iterations for Run B), the structural weight decreases rapidly since the design points are in the elastic or in the insignificant inelastic range under the design base shear (note that design base shear is a function of the period, which in turn is a function of the design variables). The convergence becomes much slower in the latter stage of the design history, as the weight of the structure decreases and the structure undergoes significant plastification while the inelastic drifts approach active. This slow convergence results from the fact that inelastic displacements are extremely sensitive to the changes in sectional sizes [32]. Therefore, it is necessary to maintain small changes in sectional sizes from

one design iteration to the next. For strategies to minimize f_2 and more details of numerical realization of the design algorithm, see [21].

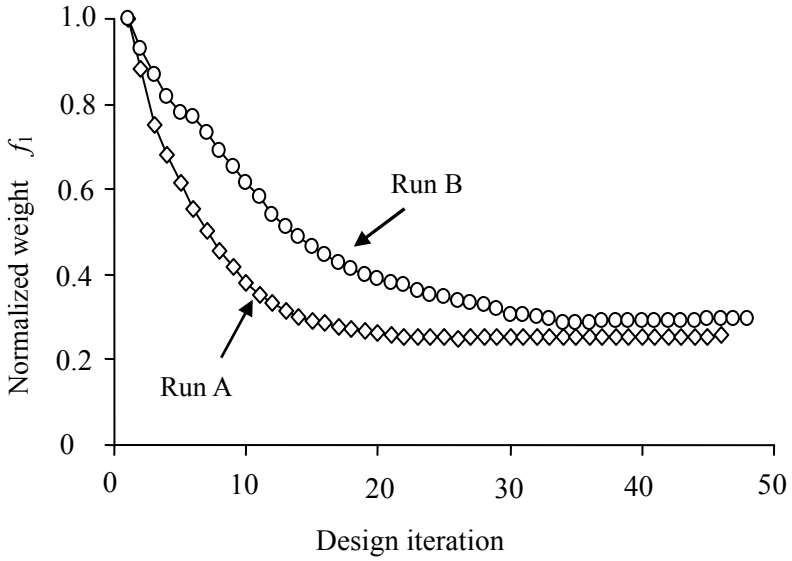

Figure 10. Design Histories of Normalized Structural Weight

7. DISCUSSIONS AND CONCLUSIONS

This paper presented a design optimization algorithm for steel moment frames under extreme earthquake loading. A pushover analysis procedure was used to evaluate seismic responses. Minimum structural cost and uniform ductility demand were taken as the design criteria. A two-stage design strategy was proposed to conduct the multi-objective optimization. In the first stage, a minimum-weight design was obtained subject to drift and side constraints (and SC/WB constraints for special moment frames). In the second stage, an optimal design with an improved ductility distribution over the minimum-weight design was obtained. This two-stage strategy eliminates the necessity of combining the two design objectives into one. The applicability and practicability of the developed optimization method was demonstrated for the design of a nine-story moment frame.

The heightwise ductility demand of a building framework is mainly dependent upon the heightwise distribution of structural stiffness (and strength) and the profile of the applied lateral inertia earthquake loads (the selection of appropriate lateral load profile is equally important to achieve the uniform ductility demand objective. However, it is beyond the scope of this paper and not discussed herein). Therefore, the proposed design formulation seeks an optimal lateral stiffness distribution for moment frames with a weight as small as possible.

It is observed from the design example that moment frames with a nearly uniform interstory drift distribution have somewhat uniform plastification over the structure height under the extreme earthquake loading. Specifically, the benefit of the SC/WB concept is that the columns are designed strong enough such that flexural yielding in beams generally dominates at multiple levels of the framework, thereby achieving a reduced likelihood of a soft or weak story and a higher level of energy dissipation. However, it is evident that SC/WB concept cannot prevent column ends from forming plastic hinges.

While pushover analysis is widely accepted as a nonlinear procedure to evaluate seismic demands, it is not shortcoming free. The pros and cons of pushover analysis have been well discussed by Krawinkler et al. [6] and Elnashai [8]. Future endeavors are desirable in two lines for applying pushover analysis in seismic design: 1) the improvement of pushover analysis in its capability of predicting seismic demands for a general structure as consistently as possible with dynamic response analysis (a pilot study in this direction can be found in [34]); and 2) the adoption of advanced analysis techniques [33] to the domain of seismic design.

8. APPENDIX: ILLUSTRATION OF EQUATION (12): $\mathbf{P} = \mathbf{D}\,\mathbf{P}_l + \mathbf{P}_g$

Consider the planar two-story moment framework shown in Figure 11. The framework has six nodes and, since each node has three degrees of freedom, the overall (gravity + lateral) nodal load vector **P** and nodal gravity load vector $\mathbf{P}_g$ each have dimension = 18×1. From Figure 11, the vector of nodal lateral loads applied at the two story levels $\mathbf{P}_l=\{P_1, P_2\}^T$ has dimension= 2×1, where loads P_1 and P_2 correspond to the 7th and 13th degrees of freedom of the structure. Therefore, the Boolean matrix **D** has dimension = 18×2 and is of the form:

$$\mathbf{D} = \begin{Bmatrix} 0 & 0 & 0 & 0 & 0 & 0 & 1 & 0 & 0 & 0 & 0 & 0 & 0 & 0 & 0 & 0 & 0 & 0 \\ 0 & 0 & 0 & 0 & 0 & 0 & 0 & 0 & 0 & 0 & 0 & 0 & 1 & 0 & 0 & 0 & 0 & 0 \end{Bmatrix}^T$$

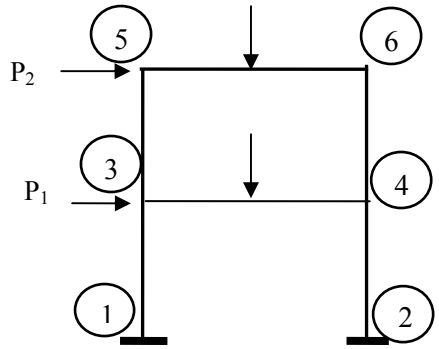

Figure 11. Two-story Moment Frame

REFERENCES

[1] BSSC, "NEHRP Recommended Provisions for Seismic Regulations for New Buildings and Other Structures (FEMA 450)", Building Seismic Safety Council, Washington DC, 2004.

[2] NRC, "National Building Code of Canada 1995", Associate Committee on National Building Code, National Research Council, Ottawa.

[3] Bruneau, M., Uang, C.M. and Whittaker, A., "Ductile Design of Steel Structures", McGraw-Hill, 389, 1998.

[4] Chopra, A.K., "Dynamics of Structures: Theory and Applications to Earthquake Engineering", Prentice Hall, 726, 2001.

[5] Federal Emergency Management Agency, FEMA-356, "Prestandard and Commentary for the Seismic Rehabilitation of Buildings", ASCE, Reston, Virginia, 2000.

[6] Krawinkler, H. and Seneviratna, G.D.P.K., "Pros and Cons of a Pushover Analysis of Seismic Performance Evaluation", Eng. Struct., 1998, Vol. 20, pp. 452-464.

[7] Hasan, R., Xu, L. and Grierson, D.E., "Pushover Analysis for Performance-based Seismic Design", Comp. Struct., 2002, Vol. 80, No. 31, pp. 2483-2493.

[8] Elnashai, A.S., "Do We Really Need Inelastic Dynamic Analysis", J. Earthquake Eng., 2002, Vol. 6, Special Issue 1, pp. 123-130.

[9] Kirsch, U., "Structural Optimization: Fundamentals and Applications", Springer-Verlag, 1993.

[10] ASCE, "Recent Advances in Optimal Structural Design", Edited by Scout B., ASCE, 2002.

[11] Ganzeri, S., Pantelides, C.P. and Reaveley, L.D., "Performance-based Design Using Structural Optimization", Earthquake Eng. Struct. Dyn., 2002, Vol. 29, pp. 1677-1690.

[12] Chan, C-M. and Zou, X-K., "Elastic and Inelastic Drift Performance Optimization for Reinforced Concrete Buildings Under Earthquake Loads", Earthquake Eng. Struct. Dyn., 2004, Vol. 33, pp. 929-950.

[13] Liu, M., Burns, S.A. and Wen, Y.K., "Multiobjective Optimization for Performance-based Seismic Design of Steel Moment Frame Structures", Earthquake Eng. Struct. Dyn., 2005, Vol. 34, pp. 289-306.

[14] Xu. L, Gong, Y. and Grierson, D.E., "Seismic Design Optimization of Steel Building Frameworks", J. Struct. Eng., ASCE, 2006, Vol. 132, No. 2, pp. 277-286.

[15] Haftka, R.T., "Integrated Nonlinear Structural Analysis and Design", AIAA Journal, 1989, Vol. 27, No. 11, pp. 1622-1627.

[16] Foley, C.M. and Schinler, D., "Automated Design of Steel Frames Using Advanced Analysis and Object-oriented Evolutionary Computation", J. Struct. Eng., 2003, Vol. 129, No. 5, pp. 648-660.

[17] Gong, Y., "Optimal Stiffness Distribution of Steel Moment Frames Under Extreme Earthquake Loading", Advances in Structural Engineering, 2005, Vol. 8, No. 6, pp. 573-584.

[18] McGuire, W., Gallagher, R.H. and Ziemian, R.D., "Matrix Structural Analysis", 2nd ed., John Wiley & Sons, 2000.

[19] Cohn, M.Z., "Analysis and Design of Inelastic Structures – Volume 2: Problems, University of Waterloo Press, Ontario, Canada, 1972.

[20] CSA, "S16-01: Limit States Design of Steel Structures", Canadian Standards Association, Ontario, Canada, 2001.

[21] Gong, Y., "Performance-based Design of Steel Building Frameworks Under Seismic Loading", PhD Thesis, University of Waterloo, Canada.

[22] Wen, Y.K. and Kang, Y.J., "Design Criteria Based on Minimum Expected Life-cycle Cost", Structural Engineering World Wide, Paper No: T132-2, Elsevier Science, 1998.

[23] AISC, "Manual of Steel Construction, Load & Resistance Factor Design", Vol. I, 2nd ed., AISC, 1994.

[24] Foutch, D.A. and Yun, S.Y., "Modeling of Steel Moment Frames for Seismic Loads", J. Construct. Steel Research, 2002, Vol. 58, pp. 529-564.
[25] AISC, "Seismic Provisions for Structural Steel Buildings", American Institute of Steel Construction, 2002.
[26] Chan, C-M., Grierson, D.E. and Sherbourne, A.N., "Automatic Optimal Design of Tall Steel Building Frameworks", J. Struct. Eng., 1995, Vol. 121, No. 5, pp. 838-847.
[27] Federal Emergency Management Agency, "Recommended Seismic Design Criteria for New Steel Moment-frame Buildings", FEMA-350, SAC Joint Venture, 2000.
[28] Arora, J.S., "Methods for Discrete Variable Structural Optimization, Recent Advances in Optimal Structural Design, Edited by Scout B, ASCE, 2002.
[29] Schmit, L.A. and Farshi, B., "Some Approximation Concepts for Structural Synthesis", AIAA Journal, 1974, Vol. 12, No. 5, pp. 692-699.
[30] Fleury, C., "Structural Weight Optimization by Dual Methods of Convex Programming", Int. J. Numer. Meth. Engng., 1979, Vol. 14, pp. 1761-1783.
[31] Gong, Y., Xu, L. and Grierson, D.E., "Performance-based Design Sensitivity Analysis of Steel Moment Frameworks Under Seismic Loading", Int. J. Numer. Meth. Engng., 2005, Vol. 63, pp. 1229-1249.
[32] Gong, Y., Xu, L. and Grierson, D.E., "Sensitivity Analysis of Steel Moment Frames Accounting for Geometric and Material Nonlinearity", Comp. & Struct., 2006, Vol. 84, No. 7, pp. 462-475.
[33] Chan, S.L., "Non-linear Behaviour and Design of Steel Structures", J. Construct. Steel Research, 2001, Vol. 57, pp. 1217-1231.
[34] Grierson, D.E., Gong, Y. and Xu, L., Optimal Performance-based Seismic Design Using Modal Pushover Analysis", J. Earthquake Eng., 2006, Vol. 10, No. 1, pp. 73-96.